Hindawi
Advances in Condensed Matter Physics
Volume 2018, Article ID 8720169, 5 pages
https://doi.org/10.1155/2018/8720169

Research Article

Enhanced Photoluminescence in Gold Nanoparticles Doped Homogeneous Planar Nematic Liquid Crystals

Chi-Huang Chang,[1,2] Rong-Ji Lin,[3,4] Chuen-Lin Tien,[3,5] and Shang-Min Yeh[6]

[1] *Department of Ophthalmology, Chung Shan Medical University Hospital, Taichung 402, Taiwan*
[2] *Department of Medicine, Chung Shan Medical University, Taichung 402, Taiwan*
[3] *Ph.D. Program of Electrical and Communications Engineering, Feng Chia University, Taichung 40724, Taiwan*
[4] *Department of Optometry, Da-Yeh University, Changhua 515, Taiwan*
[5] *Department of Electrical Engineering, Feng Chia University, Taichung 40724, Taiwan*
[6] *Department of Optometry, Central Taiwan University of Science and Technology, Taichung 40601, Taiwan*

Correspondence should be addressed to Shang-Min Yeh; optom.yap@gmail.com

Received 7 May 2018; Accepted 19 July 2018; Published 5 August 2018

Academic Editor: Daniel Ho

This study reported the photoluminescence (PL) of gold nanoparticles (GNPs) doped planar nematic liquid crystals (NLCs) and observed around 64% enhancement in PL intensity with suitable doping amounts of GNPs in liquid crystals 5CB. The enhancement in PL intensity has been attributed to the increased surface area from GNPs, which results in increased emissions due to the increased scattering of excitation. The subsequent decay of PL intensity with doping more amounts of GNPs in liquid crystals 5CB was due to the aggregation of the GNPs, which resulted in decayed emissions due to the decay of the scattering of excitation. The concentration and the size of GNPs, as well as the orientation of the LCs' director, with respect to the excitation, which depend on the intensity of the PL, were also investigated.

1. Introduction

Research in the field of liquid crystals (LCs) has developed due to its imposing properties [1–4], especially, the physical and chemical properties, which are widely applied in liquid-crystal displays (LCDs). The main drawback of liquid-crystal displays (LCDs) is low brightness, which is due to the use of absorbing color filters and dichroic sheet polarizers. The luminescence of LCD is a possible method to improve the low brightness issue [5–7]. The problem of making a luminescent LCD is that light emissions in the visible region of the electromagnetic spectrum are lessened by using pure LC materials [8–10]. The enhanced luminescence of the LC materials may definitely realize the emissive LCDs [11–13]. Doping metal materials or metal nanoparticles (NPs) in LCs have attracted much attention due to the enhanced electro-optical properties of the doped LC materials. Palewska et al. investigated the influence of electric field on photoluminescence of lanthanide-doped nematic liquid crystals and obtained a highly resolved luminescence and luminescence excitation spectra [14]. Kumar et al. reported the characterization and photoluminescence (PL) in gold nanoparticles doped ferroelectric liquid crystals and obtained enhancement in PL intensity [3]. Kuo et al. reported the enhancement of photoluminescence (PL) intensity of NLC doped with silver NPs [15]. Tanabe et al. reported the full-Color tunable photoluminescent ionic liquid crystals based on tripodal pyridinium, pyrimidinium, and quinolinium salts [16]. Lu et al. reported the electrically switchable photoluminescence of fluorescent-molecule-dispersed liquid crystals [17]. This study investigates photoluminescence (PL) in GNPs doped homogeneous planar NLCs and obtains about 64% enhancement in PL intensity with doping suitable amounts of GNPs in liquid crystals 5CB.

2. Preparation of Sample and Experimental Setup

The materials adopted in this work are nematic LCs (NLCs), 5CB (from Merck), and GNPs with diameters of 13 nm,

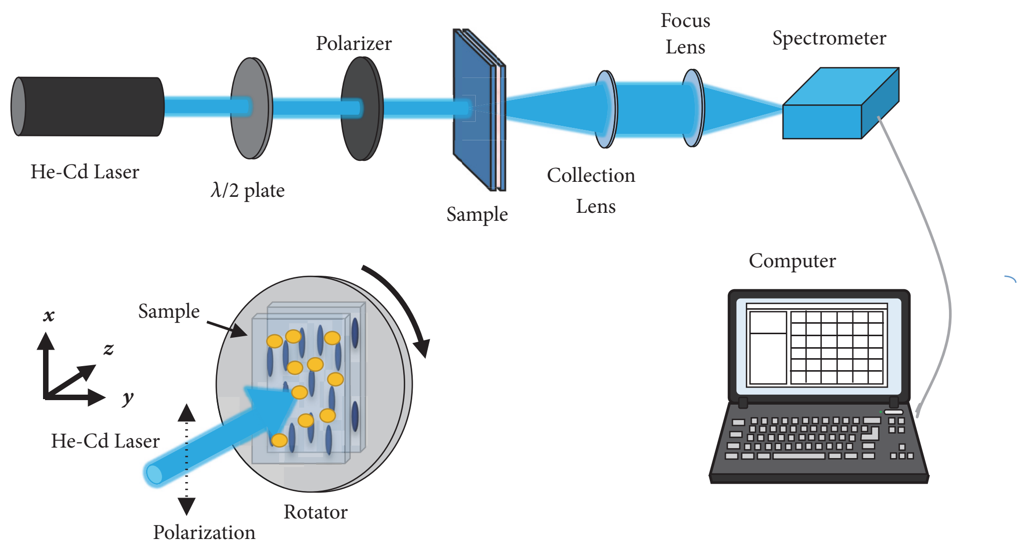

FIGURE 1: Experimental setup for measuring the PL spectra of the enhanced photoluminescence in GNPs doped homogeneous planar NLCs.

32 nm, and 56 nm (the concentrations of GNPs are $5*10^9$ *particles/ml*, $9*10^9$ *particles/ml*, $1.3*10^{10}$ *particles/ml*, $1.8*10^{10}$ *particles/ml*, and $2.5*10^{10}$ *particles/ml*). These materials are uniformly mixed and capillarity injected into the sample cell, which is assembled from two indium-tin-oxide-coated glass slides separated by two 5.4μm-thick plastic spacers. The homogeneous planar alignment of the NLCs is accomplished unidirectionally by rubbing polyimide on the inner surfaces of the two glass substrates.

Figure 1 depicts the experimental setup for the investigation of the enhanced photoluminescence in GNPs doped homogeneous planar NLCs, where the CW helium-cadmium laser (wavelength: 325 nm, power: 1 mW) is focused on the sample cell. A half-wave plate ($\lambda/2$ for 325 nm) and a polarizer are placed in front of the sample cell to maintain the excitation power of 1 mw, the polarization of the excitation beam is fixed parallel to the x-axis, and the director of the NLCs is rotated every 15 degrees from x-axis (0 degree) to y-axis (90 degree). The spectra of photoluminescence (PL) are measured with a spectrometer and analyzed by computer.

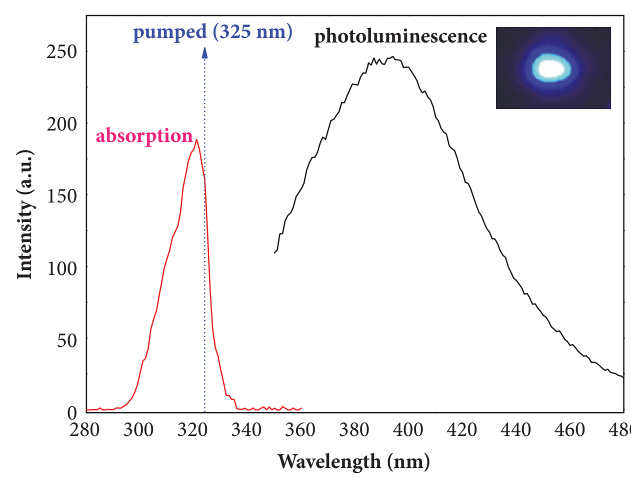

FIGURE 2: The experimental absorption and fluorescence emission spectra of the pure NLCs cell and the image of the fluorescence emission under the pumped helium-cadmium laser operated at 325 nm.

3. Results and Discussions

Figure 2 shows the experimental absorption and fluorescence emission spectra of the pure NLCs cell (without doping GNPs). The absorption spectrum covered from 288 to 340 nm and the photoluminescence spectrum was recorded from 350 nm to 500 nm, respectively. The maxima of the absorption and fluorescence emissions are about 321 and 394 nm, respectively. The inset of Figure 2 shows the image of the fluorescence emission under the pumped helium-cadmium laser, which is operated at 325 nm.

Figure 3 shows the photoluminescence spectra of GNPs doped homogeneous planar NLCs, where the concentrations of GNPs are $5*10^9$ *particles/ml*, $9*10^9$ *particles/ml*, $1.3*10^{10}$ *particles/ml*, $1.8*10^{10}$ *particles/ml*, and $2.5*10^{10}$ *particles/ml*, respectively; and the gold nanoparticle size is 13 nm in diameter. Figure 3(a) shows that the PL intensity gradually increased with the increased amount of GNPs per ml in NLCs. In the pure NLCs, the peak value of the PL intensity is around 250.4; the peak values of PL intensities are 303.5, 324.4, and 372.8, respectively, which correspond to doping GNPs with the concentrations of $5*10^9$ *particles/ml*, $9*10^9$ *particles/ml*, and $1.3*10^{10}$ *particles/ml*. The ratio between the maximum and minimum of peak intensity is ~1.49, meaning 49% enhancement in PL intensity with suitable concentrations of $1.3*10^{10}$ *particles/ml*.

Figure 3(b) shows that PL intensity gradually decayed with the increased amount of GNPs per ml in NLCs. The peak values of PL intensity are 372.8, 319.3, and 275.0, respectively, which correspond to doping GNPs with concentrations of $1.3*10^{10}$ *particles/ml*, $1.8*10^{10}$ *particles/ml*, and $2.5*10^{10}$ *particles/ml*.

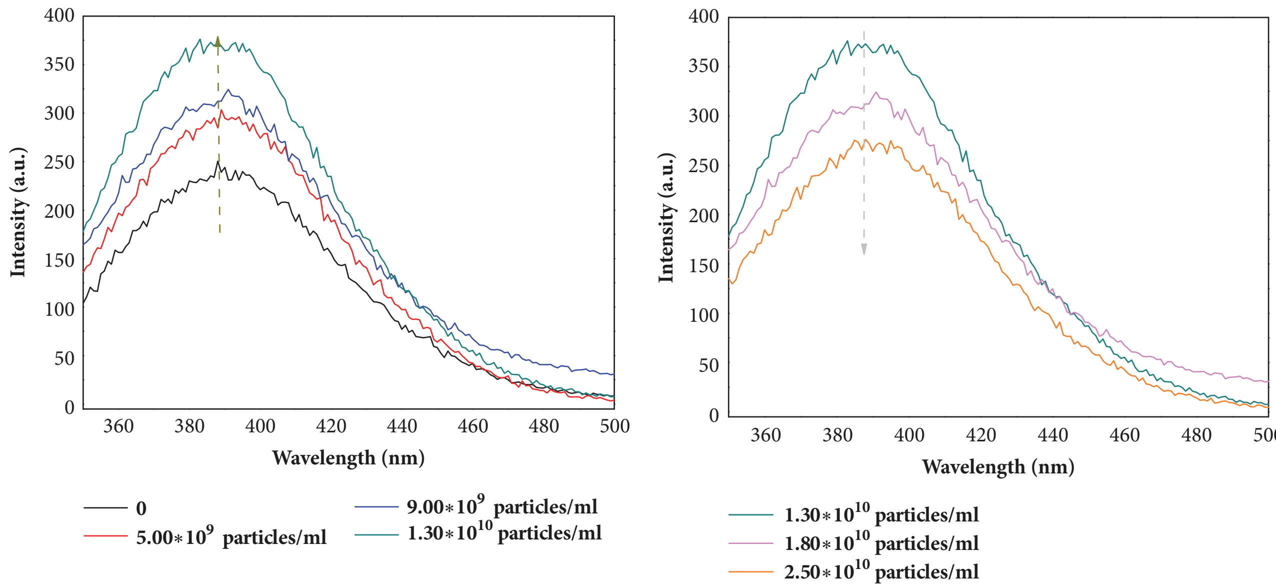

(a) (b)

Figure 3: The photoluminescence spectra of GNPs doped homogeneous planar NLCs, where the concentrations of GNPs are (a) 0, $5*10^9$, $9*10^9$, and $1.3*10^{10}$ *particles/ml*, respectively, and (b) $1.3*10^{10}$, $1.8*10^{10}$, and $2.5*10^{10}$ *particles/ml*, respectively, and the gold nanoparticle size is 13 nm in diameter.

The enhancement of photoluminescence intensity is attributed to the increased surface area from the GNPs, which strengthens the multiple reflections of the excitation beam and results in the local surface plasmon resonance effect. This effect becomes more obvious with suitable doping concentrations of GNPs in the NLCs (NLCs). The decay of PL intensity is attributed to the aggregation of the GNPs, which cause the surface area to decrease, resulting in the reduction of the energy transfer effect between NLCs and GNPs, and this effect leads to the decrease of PL intensity.

Figure 4 shows the peak intensity of PL emissions versus concentrations of GNPs with diameter sizes of 13 nm, 32 nm, and 56 nm. The peak intensity of the PL emission gradually increases in the range of concentration from 0 (pure NLCs) to $1.3*10^{10}$ *particles/ml*. The fluorescence is enhanced by the scattering of the excitation beam due to the increased surface area of GNPs. At the same concentration of gold nanoparticles (lower than $1.3*10^{10}$ *particles/ml*), the peak intensity of PL emission is stronger for 13 nm gold particles. This is because the smaller nanoparticles have larger surface areas, which causes the multiple reflections and scattering of the excitation beam. As the concentration of GNPs is larger than $1.3*10^{10}$ *particles/ml,* the peak intensity of the PL emission for a diameter size of 13 nm gradually decreases; instead, it increases the PL emissions for 32 nm and 56 nm. The smaller nanoparticles are aggregated, which reduces the surface areas, and aggregation may disrupt the ordering state of the liquid-crystal alignment. The increasing PL emissions for 32 nm and 56 nm diameters are due the gradually increased surface areas, which result in multiple reflections and scattering of the excitation beam. For GNPs of 32 nm, the peak intensity of the PL emission gradually decays as the concentration of GNPs becomes larger than $1.8*10^{10}$ *particles/ml*. This is because the aggregation of the nanoparticles reduces PL intensity. For GNPs of 32 nm, the peak intensity gradually increases with the increased concentration of GNPs; thus, decreased PL emissions can be expected, as the concentration of nanoparticles is sufficient.

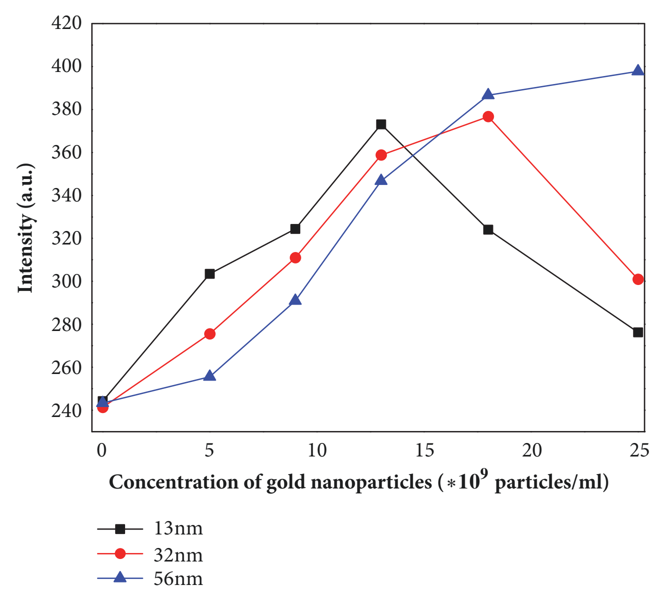

Figure 4: The peak intensity of PL emission versus concentrations of GNPs with diameter sizes of 13 nm, 32 nm, and 56 nm.

Figure 5 shows the peak intensity of the PL emission of pure NLCs and doping GNPs versus the rotational degree of NLCs' director, where the concentration of GNPs is $1.3*10^{10}$ *particles/ml*. The polarization of the excitation beam is fixed parallel to the x-axis, and the director of the NLCs is rotated

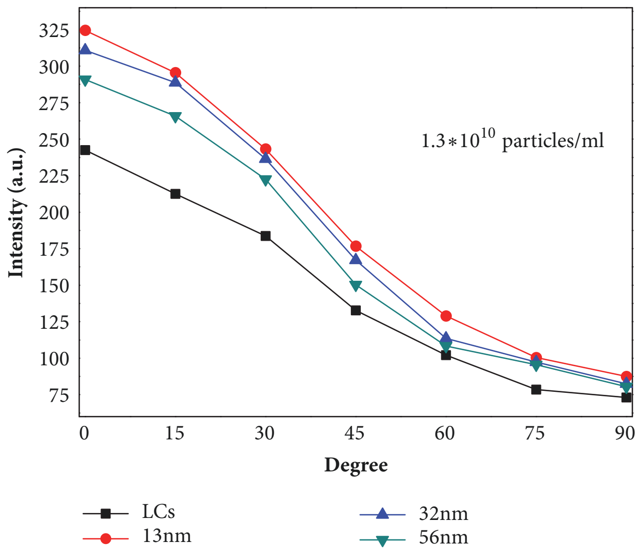

Figure 5: The peak intensity of PL emissions of pure NLCs and doping GNPs versus the rotational degree of NLCs' director, where the concentration of GNPs is $1.3*10^{10}$ *particles/ml*.

every 15 degrees from the x-axis (0 degree) to the y-axis (90 degree). All peak intensities for gold nanoparticles doping NLCs are stronger than pure NLCs', as the rotational degree is smaller than 45°. As the rotational degree gradually increases to 90°, all peak intensities decay to a similar value. The ratio between the absorption of NLCs in the x- and y-axis, denoted as A_{0°/A_{90°, is around 3.21, and the ratio between the PL intensity in the x- and y-axis, denoted as $PL_{0^\circ}/PL_{90^\circ}$, is around 3.32. These results show that the absorption of the liquid crystal critically dominates PL intensity. However, the A_{0°/A_{90° is decreased; instead, the $PL_{0^\circ}/PL_{90^\circ}$ is increased by adding gold nanoparticles in the NLCs. This result shows that the doping of GNPs causes the reduction of the ordering state of NLCs, resulting in decreased absorption. As the added GNPs provide more scattering surface area, it results in the enhancement of PL intensity.

4. Conclusions

This work investigated the photoluminescence (PL) of the GNPs doped planar NLCs. The PL intensity gradually increased with the increased amount of GNPs per ml in NLCs. The results show 64% enhancement in PL intensity with doping suitable amounts of GNPs in liquid crystals 5CB. The enhanced PL intensity is attributed to the increased surface area from the GNPs, resulting in increased emissions due to the increase of the scattering of excitation. The subsequent decay of PL intensity was attributed to the aggregation of the GNPs, as it caused decreased surface area, resulting in the reduction of the energy transfer effect between NLCs and GNPs. The size effect of GNPs was discussed, and the results show that the peak intensity of PL emission was stronger for the 13 nm gold particles at the same concentration of gold nanoparticles (lower than $1.3*10^{10}$ *particles/ml*). This is because the smaller nanoparticles have larger surface area, which causes multiple reflections and scattering of the excitation beam. By rotating the LCs' director, the results show that the absorption of the liquid crystal and the increased surface area critically dominate PL intensity.

Data Availability

The data used to support the findings of this study are included within the article.

Conflicts of Interest

The authors declare that they have no conflicts of interest.

Acknowledgments

This study was financially supported by Chung Shan Medical University Hospital (Contract no. CSH-2017-C-010).

References

[1] G. H. Brown, *Advances in Liquid Crystals*, Academic Press, London, UK, 444th edition, 1976.

[2] M. Čopič, J. E. Maclennan, and N. A. Clark, "Structure and dynamics of ferroelectric liquid crystal cells exhibiting thresholdless switching," *Physical Review E: Statistical, Nonlinear, and Soft Matter Physics*, vol. 65, no. 2, 2002.

[3] A. Kumar, J. Prakash, D. S. Mehta, A. M. Biradar, and W. Haase, "Enhanced photoluminescence in gold nanoparticles doped ferroelectric liquid crystals," *Applied Physics Letters*, vol. 95, no. 2, p. 023117, 2009.

[4] D. P. Singh, S. K. Gupta, T. Vimal, and R. Manohar, "Dielectric, electro-optical, and photoluminescence characteristics of ferroelectric liquid crystals on a graphene-coated indium tin oxide substrate," *Physical Review E: Statistical, Nonlinear, and Soft Matter Physics*, vol. 90, no. 2, Article ID 022501, 2014.

[5] L. Calucci, G. Ciofani, D. De Marchi et al., "Boron nitride nanotubes as T 2-weighted MRI contrast agents," *The Journal of Physical Chemistry Letters*, vol. 1, no. 17, pp. 2561–2565, 2010.

[6] F. V. Podgornov, A. M. Suvorova, A. V. Lapanik, and W. Haase, "Electrooptic and dielectric properties of ferroelectric liquid crystal/single walled carbon nanotubes dispersions confined in thin cells," *Chemical Physics Letters*, vol. 479, no. 4-6, pp. 206–210, 2009.

[7] Y.-S. Ha, H.-J. Kim, H.-G. Park, and D.-S. Seo, "Enhancement of electro-optic properties in liquid crystal devices via titanium nanoparticle doping," *Optics Express*, vol. 20, no. 6, pp. 6448–6455, 2012.

[8] Y. P. Piryatinskiĭ and O. V. Yaroshchuk, "Photoluminescence of pentyl-cyanobiphenyl in liquid-crystal and solid-crystal states," *Optics and Spectroscopy*, vol. 89, no. 6, pp. 860–866, 2000.

[9] J. W. Y. Lam, Y. Dong, J. Luo, K. K. L. Cheuk, Z. Xie, and B. Z. Tang, "Synthesis and photoluminescence of liquid crystalline poly(1-alkynes)," *Thin Solid Films*, vol. 417, no. 1-2, pp. 143–146, 2002.

[10] Y. P. Piryatinskiĭ, O. V. Yaroshchuk, L. A. Dolgov, T. V. Bidna, and D. Enke, "Photoluminescence of liquid-crystal azo derivatives in nanopores," *Optics and Spectroscopy*, vol. 97, no. 4, pp. 537–542, 2004.

[11] S. Kaur, S. P. Singh, A. M. Biradar, A. Choudhary, and K. Sreenivas, "Enhanced electro-optical properties in gold nanoparticles

doped ferroelectric liquid crystals," *Applied Physics Letters*, vol. 91, no. 2, p. 023120, 2007.

[12] T. Härtung, P. Reichenbach, and L. M. Eng, "Near-field coupling of a single fluorescent molecule and a spherical gold nanoparticle," *Optics Express*, vol. 15, no. 20, pp. 12806–12817, 2007.

[13] J. Zhang and J. R. Lakowicz, "Enhanced luminescence of phenyl-phenanthridine dye on aggregated small silver nanoparticles," *The Journal of Physical Chemistry B*, vol. 109, no. 18, pp. 8701–8706, 2005.

[14] K. Palewska, A. Miniewicz, S. Bartkiewicz, J. Legendziewicz, and W. Strek, "Influence of electric field on photoluminescence of lanthanide-doped nematic liquid crystal," *Journal of Luminescence*, vol. 124, no. 2, pp. 265–272, 2007.

[15] S.-Y. Huang, C.-C. Peng, L.-W. Tu, and C.-T. Kuo, "Enhancement of luminescence of nematic liquid crystals doped with silver nanoparticles," *Molecular Crystals and Liquid Crystals*, vol. 507, pp. 301–306, 2009.

[16] K. Tanabe, Y. Suzui, M. Hasegawa, and T. Kato, "Full-color tunable photoluminescent ionic liquid crystals based on tripodal pyridinium, pyrimidinium, and quinolinium salts," *Journal of the American Chemical Society*, vol. 134, no. 12, pp. 5652–5661, 2012.

[17] H. Lu, L. Qiu, G. Zhang et al., "Electrically switchable photoluminescence of fluorescent-molecule-dispersed liquid crystals prepared via photoisomerization-induced phase separation," *Journal of Materials Chemistry C*, vol. 2, no. 8, pp. 1386–1389, 2014.